JOURNAL OF SPACECRAFT AND ROCKETS
Vol. 37, No. 5, September–October 2000

Deep Space One Investigations of Ion Propulsion Plasma Environment

J. Wang* and D. E. Brinza†
Jet Propulsion Laboratory, California Institute of Technology, Pasadena, California 91109
D. T. Young‡
Southwest Research Institute, San Antonio, Texas 78228
J. E. Nordholt§
Los Alamos National Laboratory, Los Alamos, New Mexico 87545
J. E. Polk¶ and M. D. Henry**
Jet Propulsion Laboratory, California Institute of Technology, Pasadena, California 91109
R. Goldstein†† and J. J. Hanley‡‡
Southwest Research Institute, San Antonio, Texas 78228
and
D. J. Lawrence§ and M. Shappirio§§
Los Alamos National Laboratory, Los Alamos, New Mexico 87545

Deep Space One (DS1) is the first interplanetary spacecraft operated on solar electric propulsion. One of the primary investigations of DS1 is to characterize ion propulsion-induced plasma interactions and their effects on spacecraft and solar wind measurements based on two plasma diagnostic packages. The first in situ measurements of an ion propulsion-induced plasma environment obtained from an interplanetary spacecraft are reported. Analysis of the measurements reveals interesting correlations between the induced charge-exchange plasma environment and thruster operating conditions. Sensors near the thruster exit measured charge-exchange ions with a number density of $\sim 10^6$ cm^{-3} and a current density of $\sim 10^{-7}$ A/cm^{-2} under typical thruster operating conditions, a result in good agreement with preflight predictions based on computer particle simulations. Observations on the opposite side from the thruster suggest that the dominant factor for charge-exchange ion backflow is the potential distribution surrounding the spacecraft rather than the charge-exchange ion production rate.

Nomenclature

A_n	=	ion optics flow-through area
E_b, E_{cex}	=	beam ion energy and charge-exchange ion energy, respectively
I_b, I_{cex}	=	beam ion current and charge-exchange ion current, respectively
J_{b0}	=	average beam ion current density at the thruster exit
J_{cex}	=	charge-exchange ion current density
$\dot{m}_d$, $\dot{m}_m$, $\dot{m}_c$	=	discharge chamber flow rate, main flow rate, and cathode flow rate, respectively
m_{Xe}	=	xenon atom mass
$\dot{N}_n$	=	neutral Xe particle flux
n_{b0},n_{n0}	=	average number density at the thruster exit for the beam ions and the neutrals, respectively
n_{cex}	=	charge-exchange ion number density at the ion propulsion diagnostic subsystem (IDS) location
n_{cex0}	=	average number density at the thruster exit for the charge-exchange ions
q	=	electric charge
T_e	=	electron temperature
v_b, v_{cex}	=	beam ion drift velocity and charge-exchange ion velocity, respectively
η_d	=	discharge propellant efficiency
σ_{cex}	=	charge-exchange collision cross section
Φ_{IDS}	=	local plasma potential at the IDS location
Φ_p	=	plasma potential within the plume
Φ_{scg}	=	potential of the spacecraft ground

Received 9 September 1999; revision received 1 March 2000; accepted for publication 16 March 2000.

*Senior Member of Engineering Staff, Advanced Propulsion Technology Group, MS 125-109. Member AIAA.
†Senior Systems Engineer, Measurement, Test, and Engineering Support Section, MS 125-177.
‡Institute Scientist; currently Professor, Department of Atmospheric, Oceanic, and Space Sciences, University of Michigan, Ann Arbor, MI 48109-2143.
§Staff Member, Space and Atmospheric Sciences Group, MS D466.
¶Group Supervisor, Advanced Propulsion Technology Group, MS 125-109.
**Senior Systems Engineer, Avionic Systems Engineering Section, MS 198-219.
††Staff Scientist, Space Science Department.
‡‡Senior Research Engineer, Space Science Department.
§§Graduate Research Assistant, Space and Atmospheric Sciences Group, MS D466.

I. Introduction

NASA's new millennium Deep Space One (DS1) mission marks the beginning of interplanetary missions using spacecraft operated with solar electric propulsion. The DS1 spacecraft was launched on 24 October 1998. Using a 30-cm-diam xenon ion thruster as its primary propulsion system, DS1 successfully flew by asteroid 9969 Braille on 28 July 1999 and is currently on a trajectory for a possible encounter with comet Borrelly in 2001. A primary objective of DS1 is to flight validate solar electric propulsion for interplanetary science missions, including the characterization of ion propulsion-induced interactions and their effects on spacecraft payloads, subsystems, and solar wind measurements.

For a spacecraft operating with an ion thruster, there is a continuous exhaust plume composed of both the propellant efflux and the nonpropellant efflux. In ion thrusters, propellant ions are accelerated electrostatically by a system of grids to form a high-velocity beam (typically with an energy of about 1 keV). Electrons are emitted from a neutralizer for neutralization of the ion beam. The propellant

that remains un-ionized also flows out of the thruster exit at a thermal speed corresponding to the thruster wall temperature (~500 K). Charge-exchange collisions will occur between the fast moving propellant ions and the slow moving neutrals that generate slow moving ions and fast moving neutrals. (Some neutrals may also become photoionized.) The nonpropellant efflux comes from the material eroded and sputtered from the thruster and the neutralizer. A fraction of the sputtered particles can also become ionized due to charge-exchange collisions with the propellant ions or electron impact ionizations. It has long been recognized that the ion thruster plume may lead to a variety of plasma interactions and plume contaminations; hence, both science and engineering concerns have been raised over the potential effects from ion thruster operation.

One of the major concerns is the low-energy plasma generated within the plume, which is mostly due to charge-exchange collisions between the propellant ions and the neutrals. It is well known that the low-energy charge-exchange ions generated within the plume can be pushed out of the plume by the local electrostatic potential and backflow to interact with the spacecraft. Although charge-exchange plasma interactions have been a subject of extensive experimental and theoretical studies (for example, see Refs. 1–4 and references therein), there have been few comprehensive in-flight investigations due to a lack of flight opportunities.

Ion thrusters have never been flown on an interplanetary spacecraft. Although a few in-flight investigations have been attempted aboard Earth-orbiting spacecraft, such as the experiments conducted on the SERT II (Ref. 5 and 6) spacecraft in a polar orbit for a mercury ion thruster and on the ATS-6 (Ref. 7) spacecraft in geosynchronous orbit for a cesium ion thruster, almost all existing experimental data on ion thruster plume are obtained from ground tests of ion thrusters, with the majority of the data obtained for mercury and cesium ion thrusters.[1] Because the density difference between the plume and the ambient plasma greatly influences the plume potential relative to the ambient, which in turn influences the dynamics of charge exchange ions, charge-exchange plasma interactions may differ significantly in different ambient plasmas.[8] Because it is impossible to create in a vacuum tank a plasma environment similar to that under typical solar wind conditions, it is difficult to quantitatively predict ion propulsion induced plasma interactions for an interplanetary spacecraft based on ground test data.

The DS1 mission provides the first ever comprehensive in-flight investigations of ion propulsion-induced interactions and their effects. This paper reports analysis of the first in situ measurements of an ion propulsion-induced plasma environment obtained from an interplanetary spacecraft. The investigation of ion propulsion plasma environment is carried out by investigators from Jet Propulsion Laboratory (JPL), Southwest Research Institute (SwRI), and Los Alamos National Laboratory (LANL) under both DS1 mission science investigations and the NASA solar electric propulsion technology application readiness (NSTAR) program. This paper focuses on plasma measurements of the charge-exchange Xe plasma. Contamination measurements of the nonpropellant species are reported elsewhere.[9] Section II describes the DS1 ion thruster and instrumentation. Sections III and IV discuss the characterization of the ion thruster-induced plasma environment. Section V contains a summary and conclusions.

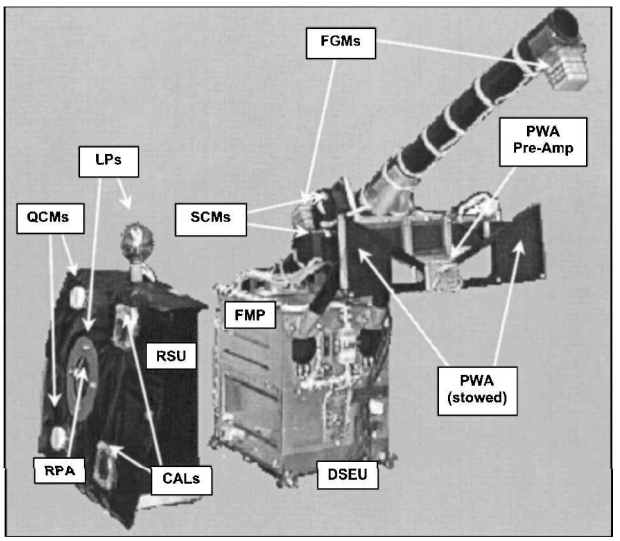

Fig. 2 IDS.

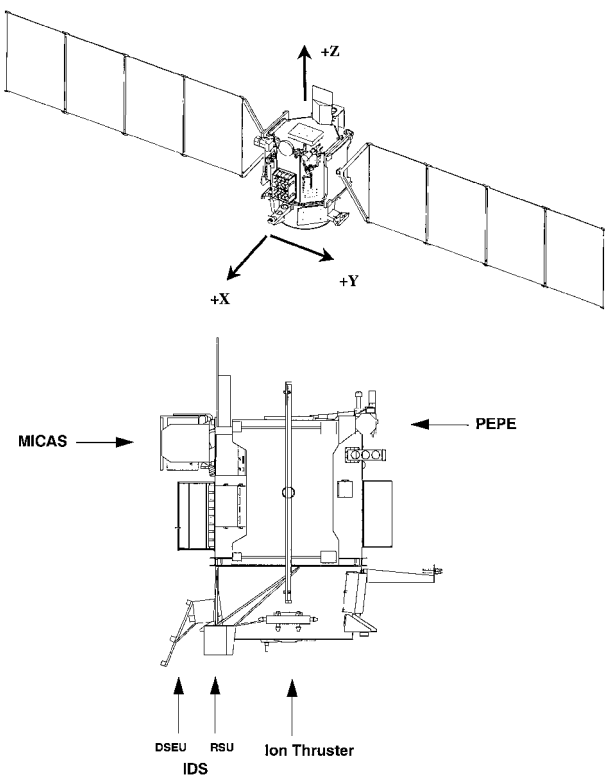

Fig. 1 DS1 spacecraft.

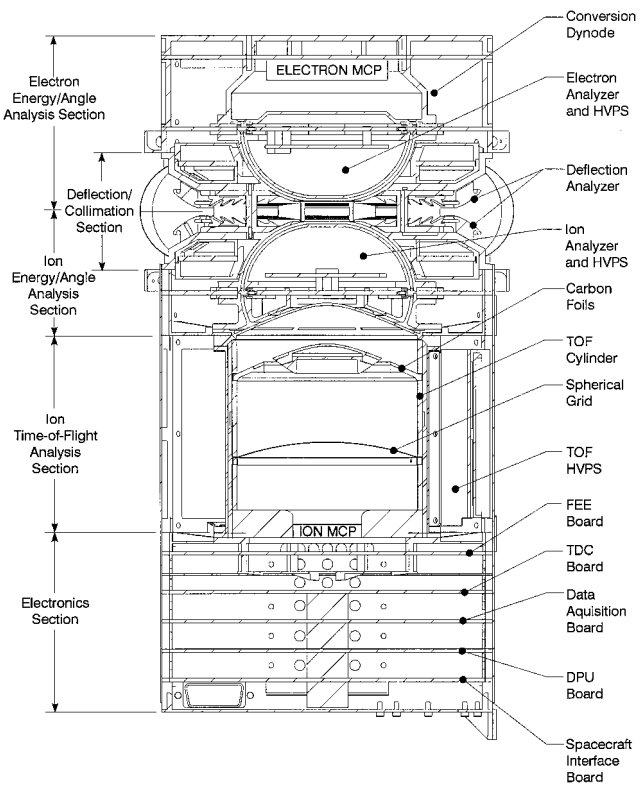

Fig. 3 Schematic diagram of PEPE.

II. Spacecraft Description

NSTAR Ion Thruster

The DS1 spacecraft is shown in Fig. 1. A detailed description of the spacecraft can be found in Ref. 10.

The flight ion propulsion system was developed under the NSTAR program, a joint JPL/NASA John H. Glenn Research Center at Lewis Field effort with industry participation from Hughes Electron Dynamics (HED), Moog, Inc., and Spectrum Astro, Inc. The 30-cm-diam xenon NSTAR thruster, fabricated by HED, has an input power range of 500–2300 W. The propellant Xe^+ ions are accelerated through a molybdenum grid to form a beam with an energy up to 1100 eV (exit beam velocity of $v_b \simeq 3.5 \times 10^6$ cm/s) and a current up to 1.8 A. At full thrust level, the thruster produces a thrust of 92 mN and a specific impulse of about 3100 s. The propellant ions form a divergent beam with a divergence half-angle of about 15–20 deg due to the curvature of the thruster exit surface. The ion beam is kept quasi neutral by electrons emitted from the neutralizer. The propellant that remains un-ionized flows out of

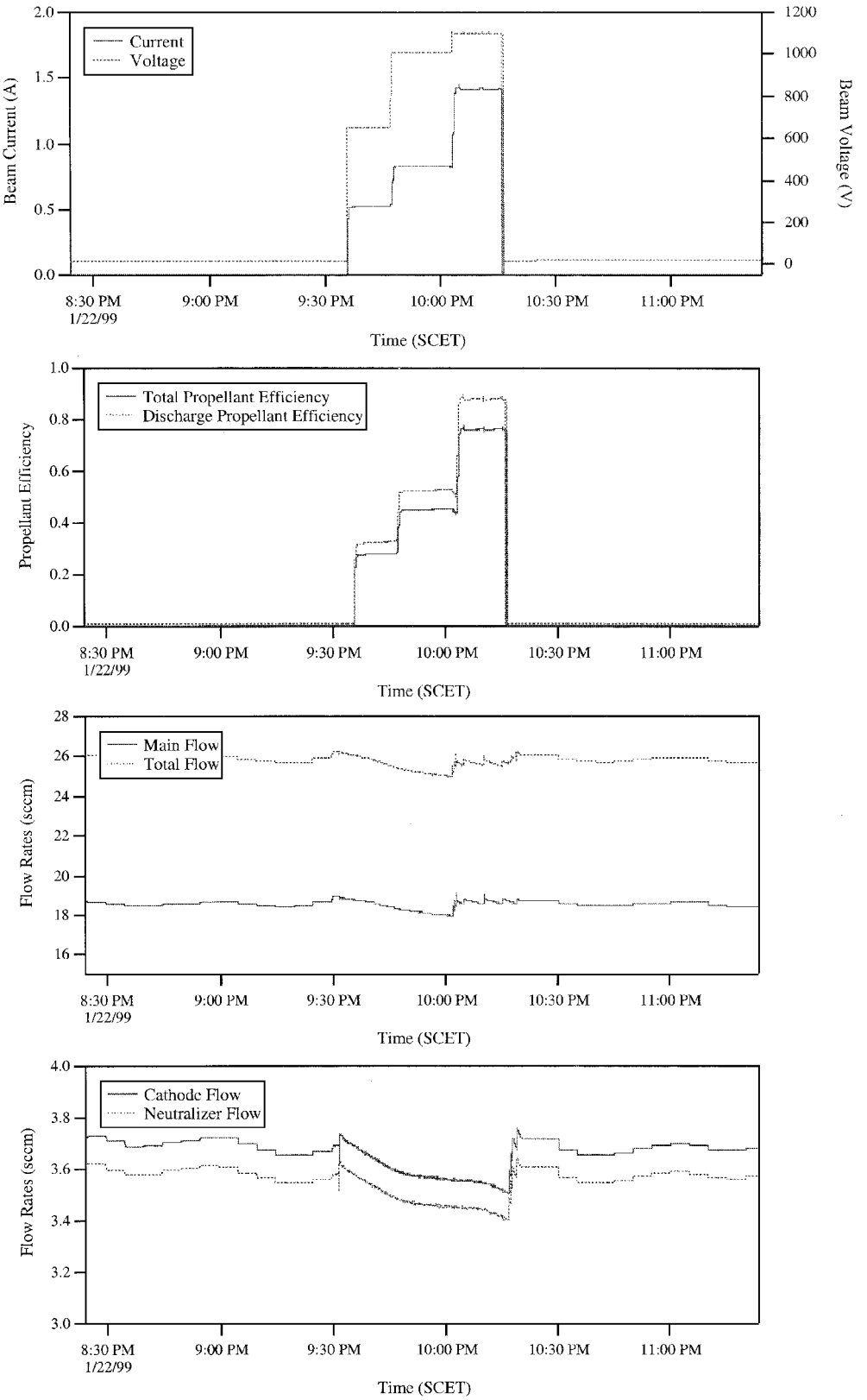

Fig. 4 Thruster parameters obtained from DS1 flight data for S-peak, 22 January 1999.

the thruster exit in free molecular flow with a thermal speed corresponding to the thruster wall temperature of ~500 K (0.04 eV). The density of the neutral plume typically remains quasi steady due to the low charge-exchange collision rate. A detailed description of the in-flight validation of the NSTAR ion thruster is discussed in Ref. 11.

Instrumentation

DS1 carries two science instrument packages, the miniature integrated camera and spectrometer (MICAS) and the plasma experiment for planetary exploration (PEPE), and one ion propulsion diagnosis package, the ion propulsion diagnostic subsystem (IDS). Ion propulsion related investigations are based on IDS and PEPE measurements. IDS is located near the ion thruster exit. PEPE is located on the upper spacecraft surface at the opposite end from the thruster (see Fig. 1).

IDS

The IDS is an integrated, comprehensive set of diagnostics designed to characterize ion propulsion-induced environments and contaminations. IDS was developed by the NSTAR project at JPL, as part of the NSTAR ion propulsion system. IDS, shown in Fig. 2, has two interconnected hardware units: the diagnostics sensors electronics unit (DSEU) and the remote sensors unit (RSU) and integrates a suite of 12 diagnostic sensors. The plasma environment is measured by a retarding potential analyzer, a planar langmuir probe, and a spherical langmuir probe. The contamination environment is monitored by two quartz crystal microbalances and two calorimeters. Electrostatic and electromagnetic noise measurements are made by a plasma wave antenna and a search coil magnetometer. Magnetic field measurements are made by two flux gate magnetometers. The two flux gate magnetometers are provided by the Technical University of Brunswick, and the plasma wave antenna is provided by TRW, Inc. The rest of the sensors are built at JPL. The contamination and plasma sensors are mounted on the RSU and the field sensors are mounted on the DSEU.

As the focus of this paper is on the induced plasma environment, we will only analyze data obtained from the IDS retarding potential analyzer (RPA) and the IDS planar langmuir probe (LP1). IDS-RPA and IDS-LP1 are collocated at about 75 cm from the thruster centerline (see Fig. 1). IDS-RPA has a voltage range of 0 to +100 Vdc and a current range of 0–100 μA. The opening to the RPA is 20 cm^2. IDS-LP1 has a voltage range from −12 to +12 Vdc and a current range from −0.5 to +40 mA. The current collecting area of IDS-LP1 is 50 cm^2.

PEPE

The PEPE is a novel state-of-the-art plasma sensor developed by SwRI and LANL. The main objectives of PEPE are to study solar wind plasma physics, cometary plasma processes, and asteroid environments and to contribute to the evaluation of ion thruster-induced plasma environment.

Figure 3 is a schematic diagram of the PEPE instrument in cutaway view showing the major elements. The main components of PEPE include miniaturized electrostatic analyzer optics and linear electric field time-of-flight mass spectrographs. PEPE simultaneously measures the differential flux of electrons and mass-resolved

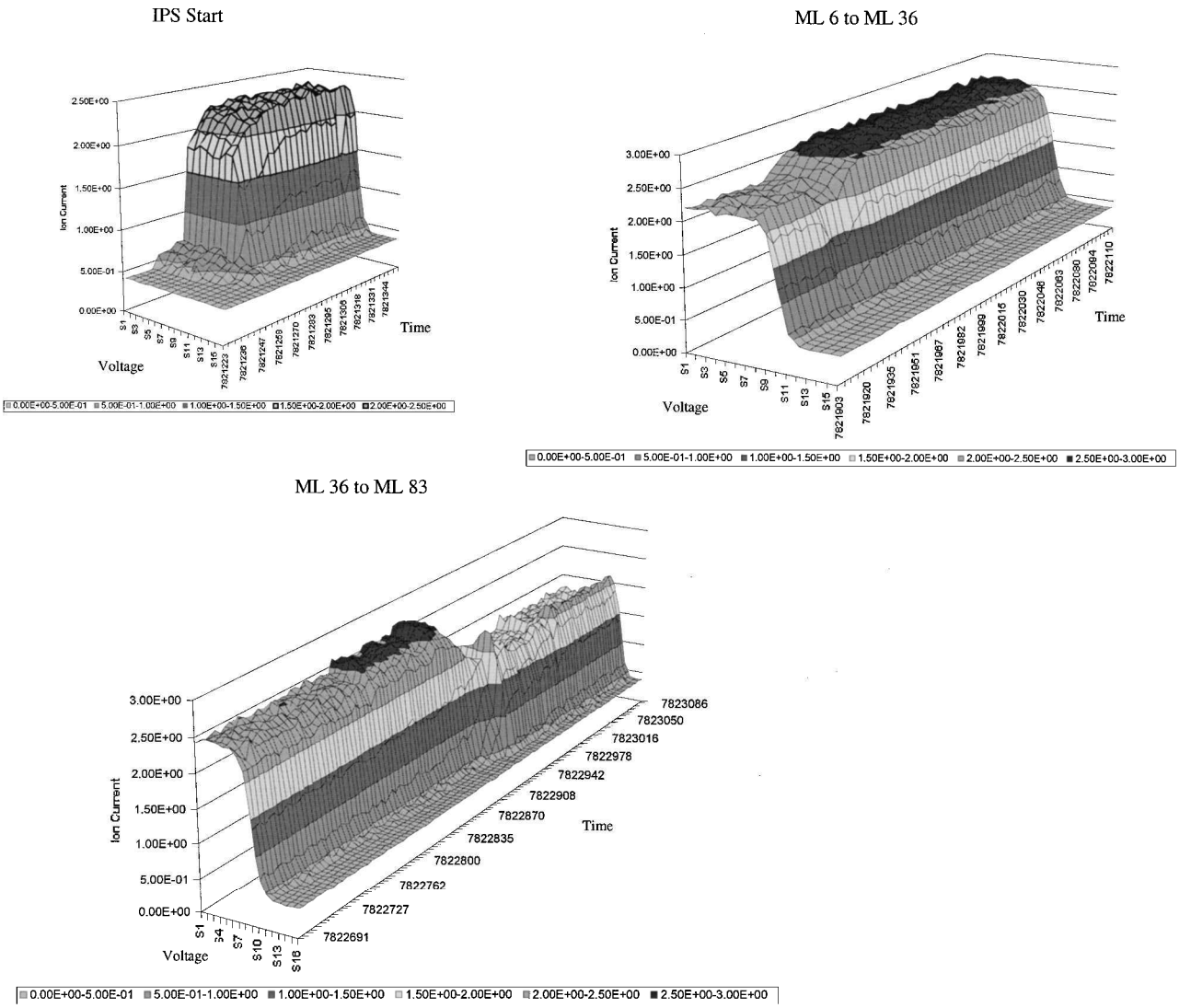

Fig. 5 Time history of IDS-RPA sweep for S-peak; time shown is in spacecraft clock starting from about 9:35 p.m.

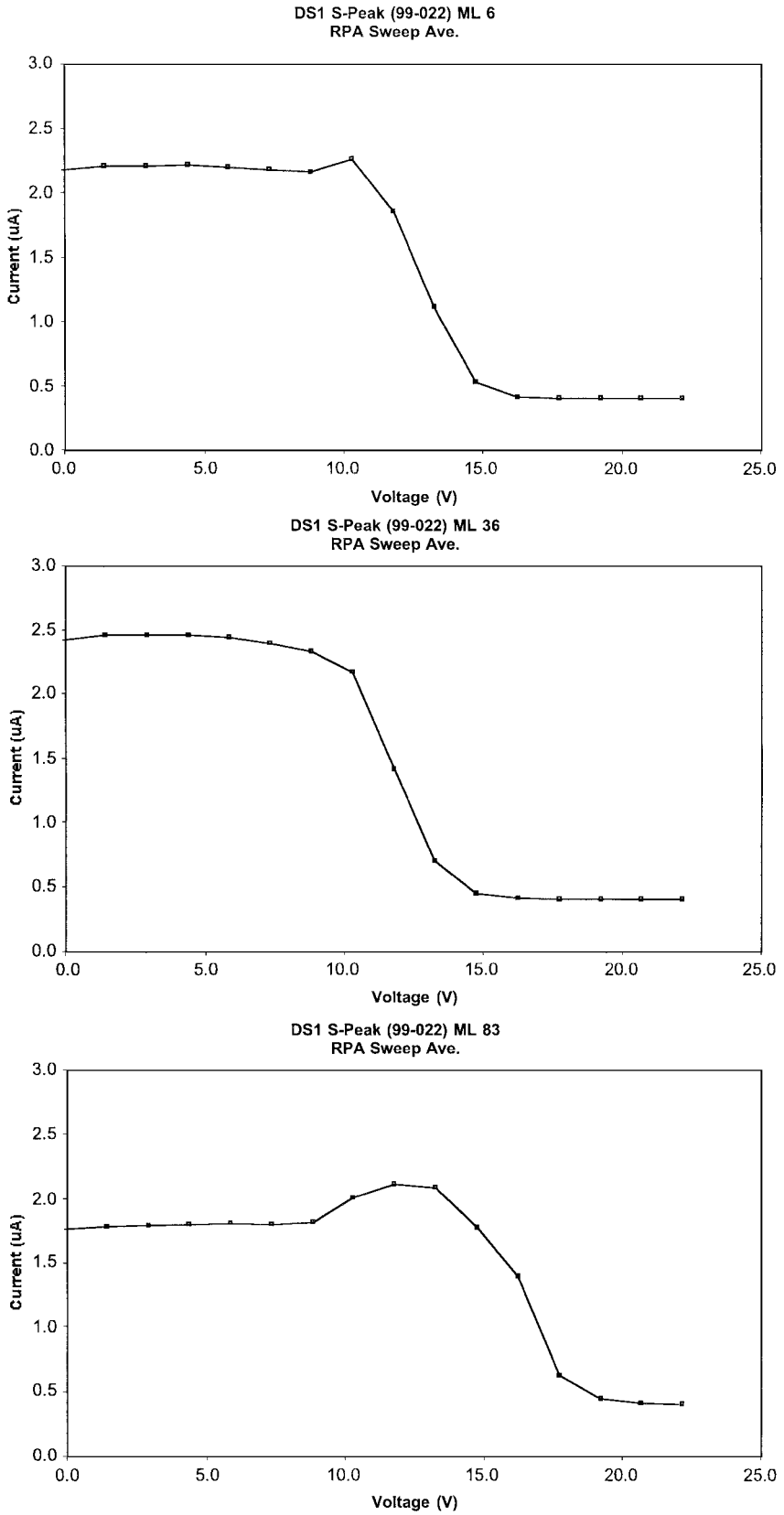

Fig. 6 IDS-RPA sweep curve averaged for each thrust level.

ions over a solid angle range of 2.8π sr and an energy/charge range of 8–33,500 eV/q. Mass/charge is resolved using a unique time-of-flight system with a mass range of 500 atomic mass unit (amu)/q and resolution $M/\delta M = 30$. Hence, the two major species emitted by the ion thruster, propellant Xe and sputtered engine material Mo, can be easily distinguished from the solar wind protons. PEPE's sensitivity is approximately 10^{-2} cm$^2 \cdot$ sr$\cdot$ eV/eV for electrons and 10^{-3} cm$^2 \cdot$ sr$\cdot$ eV/eV for ions. PEPE has an elevation angle range from -45 to $+45$ deg and an azimuthal angle of the full 360-deg range (minus spacecraft obstructions). The observed solid angle is resolved into 256 angular pixels of 5×22.5 deg for electrons and varying pixel sizes of 5×5 deg up to 5×45 deg for ions. Electrostatic deflection optics are employed to scan the PEPE field of view (FOV) by ± 45 deg in elevation angle once every 0.51 s. PEPE obtains a full three-dimensional scan in both energy and angle in about 65.5 s. PEPE data are analyzed by casting the detector counting rates

in the form of three-dimensional velocity distribution functions in phase space.

III. Characterization of Ion Thruster-Induced Plasma Environment

In this section, we present an initial characterization of the ion propulsion-induced plasma environment for DS1 based on IDS-RPA, IDS-LP1, and PEPE measurements. During the time between the initial start of the ion engine in late November 1998 and the completion of the deterministic thrusting for the encounter with asteroid Braille in July 1999, the ion propulsion system operated for a total of 1791 h at engine power levels ranging from 0.48 to 1.94 kW (Ref. 11). High-quality data were collected by IDS and PEPE for a variety of engine operating conditions. We focus on measurements obtained during a DS1 activity called S-peak. The S-peak data set is of particular interest because thrusting during S-peak reached one

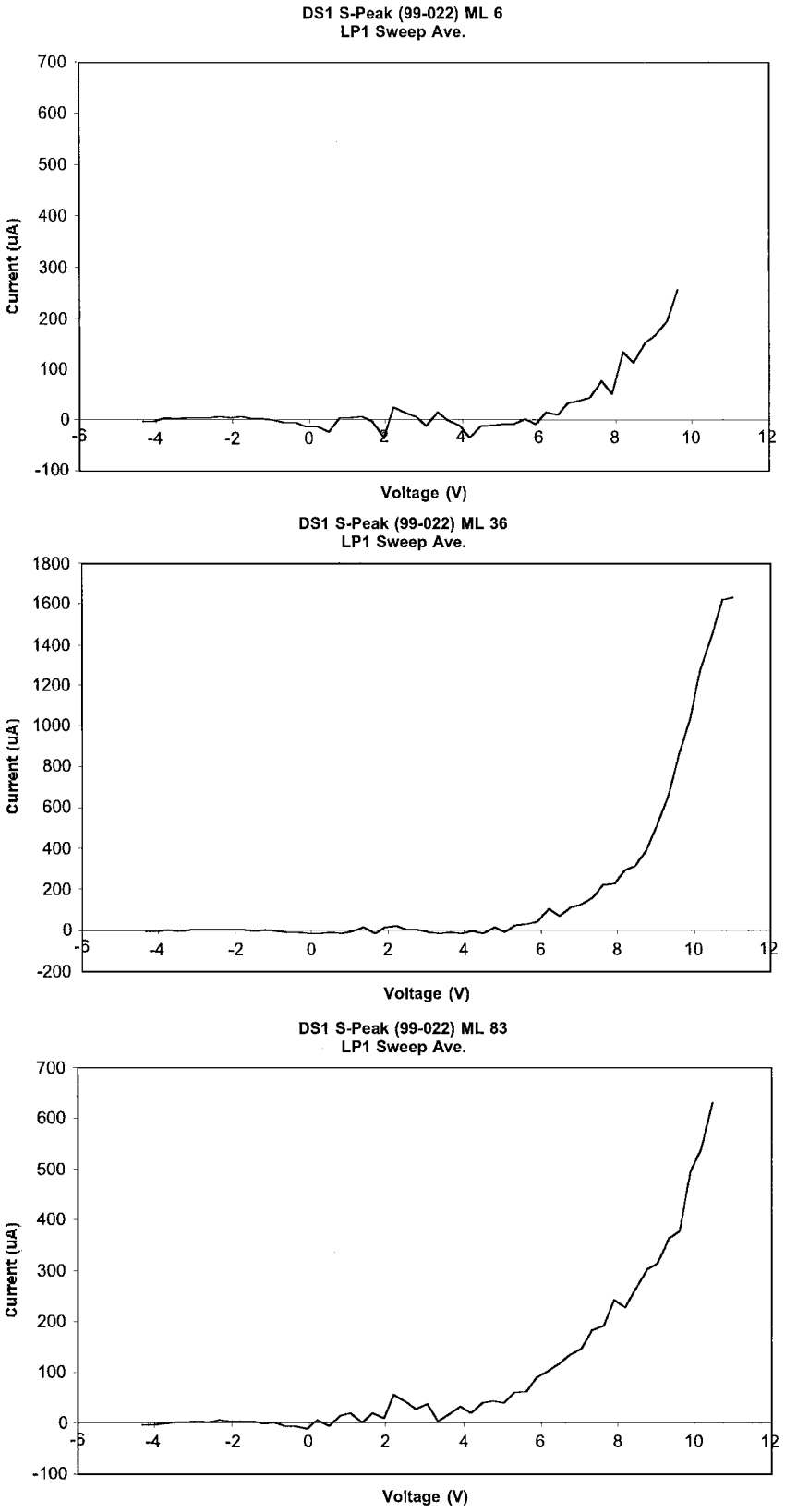

Fig. 7 IDS-LP1 sweep curve averaged for each thrust level (note scale change in middle panel).

of the highest power levels in the entire DS1 mission, which is also the highest engine power level among all of the operating conditions covered by simultaneous IDS and PEPE measurements.

Ion Thruster Operation: DS1 S-Peak

The DS1 S-peak activity occurred on 22 January 1999. S-peak is designed to determine the peak power point for the Solar Concentrator Arrays with Refractive Linear Element Technology (SCARLET) arrays. Both IDS and PEPE were operating before, during, and after the S-peak activity.

The S-peak thrusting started at 2136 Pacific daylight time (PDT). The thruster operation stepped through three thrust levels, starting at a low thrust level, then stepping to a medium thrust level, and finally a high thrust level. On the flight throttle table, the three thrust levels are defined as mission levels (ML) 6, 36, and 83, respectively. Thrusting stopped at 2217 PDT. Figure 4 shows several key thruster performance parameters obtained from flight data, including beam current and voltage, propellant efficiency, and flow rates. The values of beam current I_b, beam ion energy E_b, and discharge propellant efficiency η_d are also listed in Table 1. The specific impulses for the three thrust levels are approximately 1972, 2935, and 3189 s for ML 6, 36, and 83 respectively.[11] The engine input power ranges from 0.47 kW at ML 6–1.82 kW at ML 83. ML 83 is one of the highest power levels at which the thruster has operated during the entire DS1 mission and produces the highest specific impulse among all of the throttle levels. Because of the short S-peak time, the propellant flow had not reached an equilibrium state.

To benchmark the induced plasma environment at different thrust levels, we estimate the average charge-exchange ion production rate at thruster exit from these thruster parameters. The average charge-exchange ion production rate at the thruster exit is given by

$$\frac{\mathrm{d}n_{\mathrm{cex}0}}{\mathrm{d}t} = n_{b0} n_{n0} v_b \sigma_{\mathrm{cex}} \tag{1}$$

where n_{b0} is the average beam ion density at the thruster exit, n_{n0} the average neutral density at the thruster exit, v_b the beam ion velocity, and σ_{cex} the charge-exchange ion collision cross section.

One can estimate n_{n0} from the measured main flow rate, cathode flow rate, and the discharge propellant efficiency η_d. Assuming that the un-ionized propellant exits through the grids in free-molecular flow with a temperature close to that of the thruster discharge chamber walls, T_w, density n_{n0} can be calculated from

$$n_{n0} = \dot{N}_n \Big/ A_n \sqrt{8kT_w / \pi m_{\mathrm{Xe}}} \tag{2}$$

Table 1 S-peak thrust conditions, 22 January 1999

Thrust level	I_b, A	E_b, eV	η_d
ML 6	0.52	649	0.32
ML 36	0.82	1003	0.52
ML 83	1.40	1095	0.88

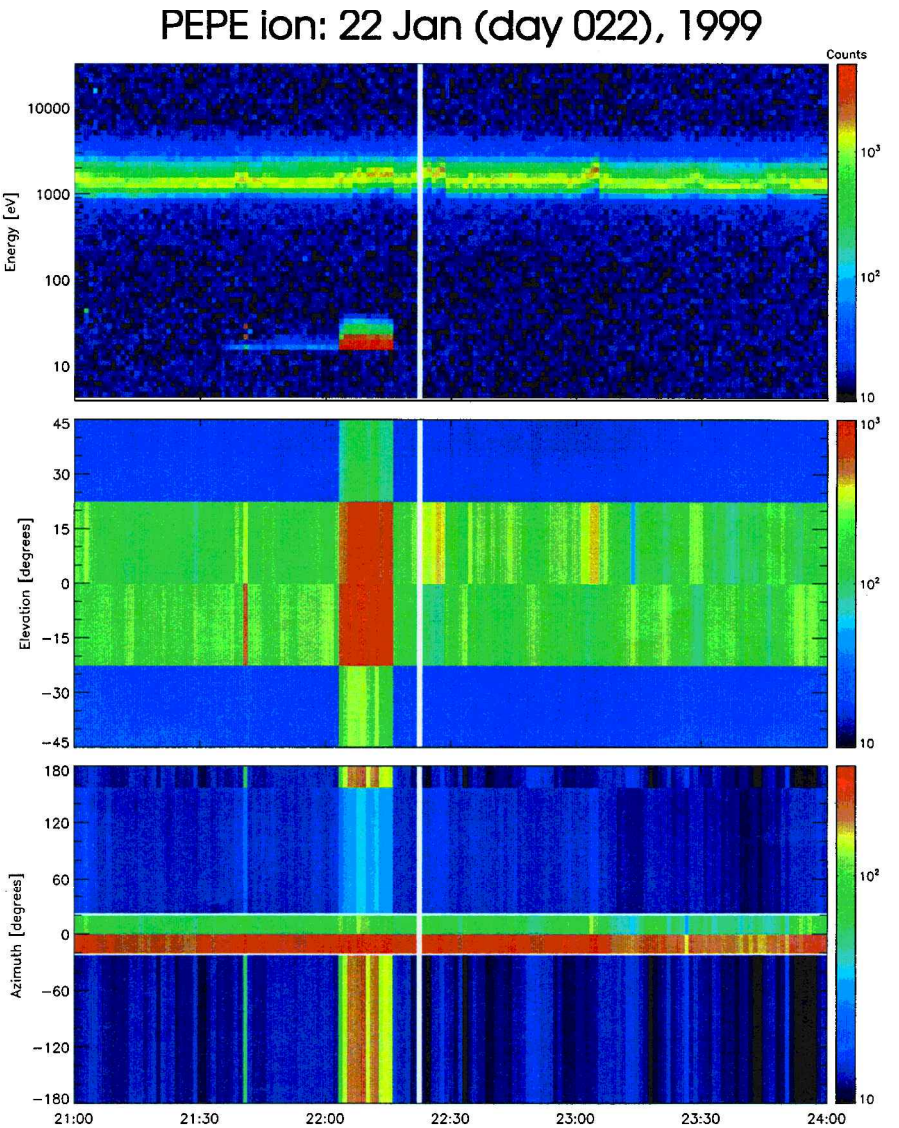

Fig. 8 Spectrogram for single ions measured by PEPE: top, ion energy per charge in eV/e; middle, ion distribution in elevation angle; and bottom, ion distribution in azimuth angle.

where $\dot{N}_n$ is the number of Xe particles per second and is converted from the discharge chamber flow rate, $\dot{m}_d = (1 - \eta_d)(\dot{m}_m + \dot{m}_c)$. A_n is the flow-through area through the grids and is about 0.24 of the thruster exit area for the NSTAR thruster. Cross section σ_{cex} can be estimated from curve fitting of the measured collision cross section for $Xe^+ - Xe$ charge-exchange[2,12]

$$\sigma_{cex} = (k_1 \ln v_b + k_2)^2 \times 10^{-16} \text{ cm}^2 \quad (3)$$

where v_b is beam ion velocity in meters per second, $k_1 = -0.8821$, and $k_2 = 15.1262$. For the three thrust levels considered, σ_{cex} ranges from 3.65×10^{-15}cm^2 for ML 6–3.37×10^{-15}cm^2 for ML 83. The calculated beam plasma density, neutral density, and the charge-exchange ion production rate near the thruster exit are listed in Table 2. Note that all of the parameters listed in Table 2 are averaged estimations at each thrust level because the thruster did not have time to reach its equilibrium condition during S-peak.

Table 2 Parameters at thruster exit for S-peak

Thrust level	J_{b0}, A/m^2	v_b, km/s	n_{b0}, 1/cm^3	$\dot{N}_n$, 1/s	n_{n0}, 1/cm^3	dn_{cex0}/dt, 1/cm^{3}s
ML 6	7.36	29.8	1.54×10^9	6.2×10^{18}	1.4×10^{12}	2.3×10^{13}
ML 36	11.6	37.0	1.96×10^9	4.3×10^{18}	0.95×10^{12}	2.4×10^{13}
ML 83	19.8	38.7	3.22×10^9	1.1×10^{18}	0.23×10^{12}	1.0×10^{13}

Charge-Exchange Plasma Measured by IDS

Figures 5–7 show the data obtained from IDS-RPA and IDS-LP1 during S-peak. Figure 5 shows the time history of the IDS-RPA sweep from before the start of ion thruster operation through thrust level ML 83. (The time in Fig. 5 is labeled by spacecraft clock.) Figure 6 shows the averaged IDS-RPA sweep curve at each thrust level. (The bumps in the curves for ML 6 and ML 83 are due to interference from the collocated IDS-LP1, which was performing voltage sweeps at the same time.) Figure 7 shows the averaged IDS-LP1 sweep curve at each thrust level.

As shown in Fig. 5, the IDS-RPA started to collect an ion current as soon as the ion thruster started firing. The sudden change in the saturated ion current corresponds to the change in thrust level. The voltages measured by the RPA and LP are all relative to the spacecraft ground. From Fig. 6, we can obtain the ion current and ion energy relative to the spacecraft potential for each thrust level. From Fig. 7, we can obtain the local plasma potential relative to the spacecraft potential and the electron temperature for each thrust level. Table 3 lists these results.

Table 3 IDS results

Thrust level	I_{cex}, μA	E_{cex}, eV	T_e, eV	$\Phi_{IDS} - \Phi_{scg}$, V
ML 6	2.2	15	1.17	6
ML 36	2.4	14	1.33	5
ML 83	1.8	19	2.09	4

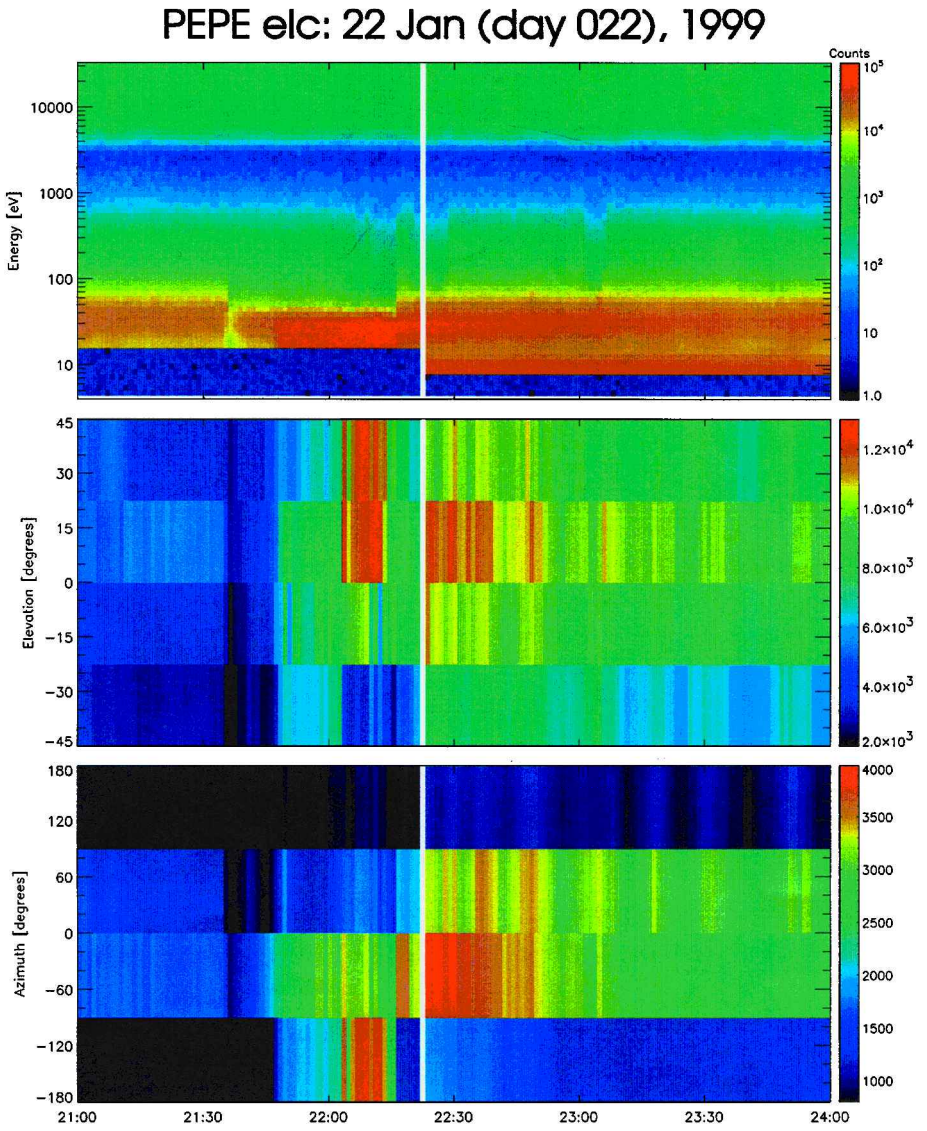

Fig. 9 Spectrogram for electrons measured by PEPE: top, electron energy; middle, electron distribution in elevation angle; and bottom, electron distribution in azimuth angle.

The observations show that the saturated ion current collected by IDS-RPA increased from ~2.2 to ~2.4 μA when the thrust level changed from ML 6 to ML 36 and decreased to ~1.8 μA when the thrust level changed from ML 36 to ML 83. The average energy (relative to spacecraft ground) of the ions collected ranges from 14 (at ML 6 and ML 36) to 19 eV (at ML 83). The local plasma potential (relative to spacecraft ground) at IDS location is from 6 (at ML 6) to 4 V (at ML 83). The local electron temperature is about 1–2 eV.

Because IDS is located well outside of the primary plume region (see Fig. 1), the ions collected by IDS-RPA are the charge-exchange ions transported outward from the primary plume. We next derive the charge-exchange ion characteristics from the IDS results. We denote Φ_p, $\Phi_{\rm IDS}$, $\Phi_{\rm scg}$ to be the average electrostatic potential inside the thruster plume, the potential at the location of IDS, and the potential of the spacecraft ground, respectively. As the charge-exchange ions originate from the very cold neutrals (temperature 0.04 eV), the ion energy measured by RPA represents the difference between the electric potential inside the plume (where these charge-exchange ions are produced) and the spacecraft ground potential, $\Phi_p - \Phi_{\rm scg}$. From the charge-exchange ion energy measured by IDS-RPA and the local plasma potential measured by IDS-LP1, we find the difference between the plume potential and the local plasma potential

$$\Phi_p - \Phi_{\rm IDS} = (\Phi_p - \Phi_{\rm scg}) - (\Phi_{\rm IDS} - \Phi_{\rm scg}) \tag{4}$$

Hence, the average energy of the charge exchange Xe^+ ions collected by IDS is $E_{\rm cex} = e(\Phi_p - \Phi_{\rm IDS})$, which gives the average Xe^+ ion velocity at the IDS location

$$v_{\rm cex} = \sqrt{2e(\Phi_p - \Phi_{\rm IDS})/m_{\rm Xe}} \tag{5}$$

From the charge-exchange ion current density measured by RPA, one finds the charge-exchange ion density at the IDS location:

$$n_{\rm cex} = J_{\rm cex}/ev_{\rm cex} \tag{6}$$

The results of the charge-exchange ion plasma environment are listed in Table 4.

We find that the current density associated with charge exchange ion outflow is about 10^{-7} A/cm^2, and the charge exchange ion density at the IDS location is about 10^6 cm^{-3}. Not surprisingly, the differences between the charge-exchange ion densities at each thrust level correlate to the changes in the charge-exchange ion production rate estimated in the preceding section. When thrust level changed from ML 6 to ML 36, an increase in the beam ion current drove up $dn_{\rm cex0}/dt$, and hence IDS-RPA observed an increase in charge-exchange ion collection. When thrust level changed from ML 36 to ML 83, even though the beam ion current increased, a more significant decrease in the neutral density due to high η_d drove down the $dn_{\rm cex0}/dt$, and hence IDS-RPA observed a decrease in charge-exchange ion collection.

The observations show that the plume potential increases significantly as beam current increases. This is not surprising. The propellant plasma plume is a mesothermal plasma, that is, $v_{ti} \ll v_b \ll v_{te}$, where v_{ti}, v_b, and v_{te} are the ion thermal velocity, ion beam velocity, and electron thermal velocity, respectively. When a high-density plasma expands into a more dilute plasma under the mesothermal process, the plasma potential decreases as the plasma density decreases. Hence, a larger density difference between the plasma source and the ambient plasma yields a higher potential at the source relative to the ambient. The observations also show that there is an increase in electron temperature as beam current increases. This is probably because the electrons emitted from the neutralizer undergo a stronger acceleration and heating from the stronger electrostatic field associated with higher plume potential. Observe that, whereas the plume potential $\Phi_p - \Phi_{\rm IDS}$ differs by 60% between the low and high thrust levels, the ratio of the plume potential to the electron temperature is relatively a constant at about $(\Phi_p - \Phi_{\rm IDS})/T_e \sim 7$.

Table 4 Induced plasma environment at IDS

Thrust level	$\Phi_p - \Phi_{\rm IDS}$, V	$(\Phi_p - \Phi_{\rm IDS})/T_e$	$J_{\rm cex}$, A/cm^2	$v_{\rm cex}$, km/s	$n_{\rm cex}$, cm^{-3}
ML 6	9	7.7	1.1×10^{-7}	3.45	2×10^6
ML 36	9	6.8	1.2×10^{-7}	3.45	2.2×10^6
ML 83	15	7.2	0.9×10^{-7}	4.46	1.2×10^6

Charge-Exchange Plasma Measured by PEPE

PEPE is located on the opposite side of DS1 from the ion thruster to minimize the effects from ion thruster operation. However, during ion thruster operation, PEPE also measured significant Xe^+ ions. As already discussed, PEPE FOV scans above and below the plane of the ecliptic and views 360 deg instantaneously in the orthogonal direction.

Figure 8 is a color spectrogram showing ion counts measured by PEPE as function of time for a time period containing S-peak on 22 January 1999. The spectrogram covers a time period from 2100 to 2400 PDT. The top panel displays ion energy per charge in electron volt per electron charge, the middle panel shows the measured ion distribution in elevation angle, and the bottom panel shows the distribution in azimuth angle (see Fig. 1). The colors correspond to the particle counting rate. The color scale on the right gives the count level logarithmically.

The band of high count level just above 1000 eV is from the solar wind protons. What is notable, however, is the high count rate beginning at about 2204 at about 15–35 eV, corresponding to the period in which IPS was operating at the ML 83 level (see Table 1). The elevation and azimuth panels show that these ions reach PEPE from the direction of the thruster beam. Spectrogram showing the time-of-flight mass spectrum response of PEPE also showed a broad count rate peak during this period, which corresponds in mass/charge to Xe^+. The energy of Xe^+ measured by PEPE corresponds to that measured by IDS-RPA during ML 83. Thus, PEPE has conclusively shown the presence of low-energy charge-exchange Xe^+ ions during ML 83.

Figure 9 is a similar color spectrogram, but for the electrons measured by PEPE. The color scale is given logarithmically in the top panel and is given linearly in the middle and bottom panels. The lower limit of electron energy sweep was normally set at 8 eV, as shown in the time period of 2230–2400, when the thruster is off. The high count near the low-energy cutoff is due largely to the photoelectron cloud surrounding the spacecraft. This is a normal occurrence in sunlight. There is another broad peak at about 30–40 eV, corresponding to the peak in the solar wind electron distribution. Ongoing PEPE investigations suggest that the second peak may also exhibit effects from differential charging caused by the SCARLET solar array. The SCARLET solar array has a potential difference of 100 V. The negative end of the solar array is grounded at the spacecraft. The wiring of the solar array is such that the solar array has an exposed edge of +50 V above spacecraft potential. Hence, the solar array could accelerate some photoelectrons into the higher energy population.

In the time period prior to 2230, the lower limit in electron energy sweep was increased to about 15 eV to avoid a possible overload of the detector because very high count rates had been measured during previous ion thruster operation. Coincident with ion thruster operation, Fig. 9 shows that the electron count rate from 15 through 30–40 eV also increases above background. This indicates that ion thruster operation also produces a low-energy electron cloud around DS1 denser than that of photoelectrons. This is apparently caused by the electrons that drift out of the plume with the outflowing charge-exchange ions to keep the charge-exchange plasma quasi neutral.

The potential of an interplanetary spacecraft is typically a few volts positive relative to the ambient due to photoelectron emission. Because PEPE's energy range starts at 8 eV for both ions and electrons, it is not possible to make an accurate estimate of the spacecraft chassis potential based on PEPE measurements because of this energy cutoff. However, Figs. 8 and 9 show little change in the energy corresponding to the peak in both the solar wind electron and proton distributions when the thruster was operating. This suggests that any change in spacecraft potential due to ion thruster operation is within the range of PEPE energy cutoff.

Figure 9 also shows that, coincident with the entire ion thruster operating period, there is a contraction from about 60 to about

40 eV in the energy spectrum for the high-energy electrons. It could be because the ion beam and charge-exchange ions significantly changed the sheath structure surrounding the spacecraft for solar wind electron collection. The exact cause of this contraction, however, is still not clear.

IV. Discussion

Recently, several computer particle simulation models have been developed for ion thruster charge-exchange plasma.[2–4,13–15] In Ref. 4, a three-dimensional electrostatic PIC code coupled with a Monte Carlo collision calculation is used to model the charge-exchange plasma from the DS1 ion thruster. They predicted that, under typical thruster operating conditions, the outflow of charge-exchange Xe^+ should lead to a Xe^+ density of $10^6 cm^{-3}$ and a Xe^+ ion current density of $10^{-7} A/cm^2$ at the IDS location. Similar results were also obtained in Refs. 13 and 14 using a two-dimensional axisymmetric finite element particle code. The IDS measurements appear to be in good agreement with these preflight predictions.

To model PEPE collection of Xe^+ ions requires one to first obtain the electric field in the vicinity of DS1 and then trace the trajectories of the Xe^+ ions from their origin in the thruster plume to PEPE's FOV. Such a calculation requires information on the distribution of spacecraft charging potential on DS1 surface. Because of the lack of such information, previous simulations[4,13,14] have not studied the detailed effects of spacecraft potential on Xe^+ surrounding DS1. Such effects could be significant for DS1 due to the 100-V SCARLET solar array, which may influence spacecraft charging as well as interaction with the charge-exchange plasma.

That PEPE observes substantial charge-exchange Xe^+ ions only during ML 83, when the charge-exchange ion current measured by IDS-RPA and the charge-exchange ion production rate are significantly lower than that for the other two thrust levels, suggests that the more important factor affecting the induced plasma environment surrounding a spacecraft is the relative potential difference between the plume and spacecraft rather than charge-exchange ion production. This can be explained by the following qualitative discussion.

The solar wind plasma density is about 1–10 cm^{-3}. The debye length under typical solar wind conditions is on the order of 10 m. Hence, except for the small area surrounding the thruster, DS1 is covered by a thick sheath, whose thickness is much larger than the spacecraft dimension. Therefore, once a charge-exchange ion is pushed out of the plume by the electric field within the plume, it will fall into the potential field of the spacecraft sheath. For a simple, qualitative discussion, we consider the spacecraft to be a spherical probe with a radius r_{sc} and a surface potential Φ_{sc}. Hence, the orbit of a charge-exchange ion in the vicinity of spacecraft will be similar to that of charged particles near an electrostatic probe in the orbital motion limited (OML) regime.[16]

Let us consider that a charge-exchange ion is generated at location 0 within the plume and subsequently pushed out from the plume at location 1 at the plume edge with a velocity transverse to the thrust direction due to the potential difference between locations 0 and 1. We denote the electrostatic potentials at locations 0 and 1 to be Φ_{p0} and Φ_{p1}, respectively. Location 1 has a distance L from the spacecraft surface along the thrust direction. We describe the particle's orbit in a spherical coordinate centered in the probe. As the charge-exchange Xe^+ is born cold, the velocity at which it leaves the plume is $v_{1\theta} = \sqrt{[2e(\Phi_{p0} - \Phi_{p1})/m]}$. Hence, this Xe^+ leaves the plume with an initial energy

$$E_1 = e\Phi_{p1} + \tfrac{1}{2}mv_{1\theta}^2 = e\Phi_{p0} \tag{7}$$

and an initial angular momentum with respect to the spacecraft center

$$\Omega_1 = m(L + r_{sc})v_{1\theta} = m(L + r_{sc})\sqrt{2e(\Phi_{p0} - \Phi_{p1})/m} \tag{8}$$

In the OML regime, the invariants of motion are the angular momentum and the total energy. Hence, once outside the plume, this Xe^+'s orbit is determined by

$$\tfrac{1}{2}mv_r^2 + \left(\Omega_1^2/2mr^2\right) + e\Phi = E_1 \tag{9}$$

If this Xe^+ is to be collected by PEPE at the opposite side of spacecraft surface, we must have

$$E_1 - \left[\left(\Omega_1^2/2mr_{sc}^2\right) + e\Phi_{sc}\right] \geq 0 \tag{10}$$

This leads to

$$\sqrt{\frac{\Phi_{p0} - \Phi_{sc}}{\Phi_{p0} - \Phi_{p1}}} \geq 1 + \frac{L}{r_{sc}} \tag{11}$$

Therefore, the necessary condition for charge-exchange ions originated from the thruster plume to backflow to the opposite side of spacecraft is that the potential difference between the plume and the spacecraft must be sufficiently larger then the potential difference within the plume.

The potential difference between plume center and plume edge, $\Phi_{p0} - \Phi_{p1}$, is mainly determined by the beam's density profile, which in turn is controlled by the curvature of the thruster acceleration grid. Hence, the critical factor will be the potential difference between the plume and spacecraft, $\Phi_{p0} - \Phi_{sc}$. IDS-RPA shows that the average plume to spacecraft potential difference during ML 83 is about 30% higher than that during ML 6 and ML 36. This may explain why PEPE measures significant Xe^+ only during ML 83 but not during ML 6 and ML 36.

V. Conclusions

For the first time, a comprehensive in-flight investigation of ion propulsion plasma interaction has been carried out, and in situ measurements of the ion propulsion-induced plasma environment surrounding an interplanetary spacecraft in the solar wind has been obtained. Initial analysis of simultaneous IDS and PEPE measurements obtained during thruster firings revealed interesting correlations between the induced plasma environment and thruster operating conditions. At a location approximately 0.75 m away from the ion thruster centerline, IDS measured a charge-exchange Xe^+ ion current density of $\sim 10^{-7}$ A/cm^2 and a charge-exchange ion density of $\sim 10^6$ cm^{-3} during ion thruster firings. These measurements are in good agreement with preflight predictions based on three-dimensional computer particle simulations.[4] The measured Xe^+ ion density near the thruster exit is five to six orders of magnitude larger than the solar wind plasma density. The quantitative differences in the measured Xe^+ density at different thrust levels correlates with the charge-exchange ion production rate estimated from thruster data. IDS measurements also show that the plume potential will increase significantly as the beam current increases. This is because the main underlying physical process that controlles the global plume potential is the expansion of the high-density propellant plasma. Hence, the plume potential relative to the ambient sensitively depends on the beam ion density.

Whereas IDS measured more charge-exchange ions during the two lower thrust levels, PEPE, which is on the opposite side of the ion thruster, observed significant Xe^+ ions only at the highest thrust level. This suggests that the dominant factor underlying charge-exchange ion backflow is the electric potential distribution surrounding the spacecraft rather than the charge-exchange ion production. A simple analysis shows that, for charge-exchange ions to backflow to the front side of an interplanetary spacecraft, the spacecraft potential needs to be sufficiently negative with respect to the plume. For DS1, it appears that charge-exchange ion backflow can occur only at high-thrust levels. PEPE measurements show that the backflow charge-exchange Xe^+ ions can be clearly distinguished from the solar wind protons and that there was little change in the solar wind proton distributions during ion thruster firings. These suggest that meaningful plasma measurements of the ambient ions can be made during ion thruster operations. Additionally, PEPE observed little change in the energy corresponding to the peak in both the solar wind proton and electron distributions during thruster firings; hence, any change in the spacecraft potential was within the PEPE energy cutoff range of ±8 V. This indicates that spacecraft charging is not significantly affected by the ion propulsion induced plasma environment.

Acknowledgments

The work at Jet Propulsion Laboratory (JPL), California Institute of Technology, was performed under a contract with NASA and was supported by NASA New Millennium Deep Space One (DS1) mission and NASA solar electric propulsion technology application readiness (NSTAR) project. The work at Southwest Research Institute (SwRI) was supported by NASA JPL Contracts 960619 and 960439 and SwRI internal research funding for the development of the plasma experiment for planetary exploration (PEPE) instrument and by NASA JPL Contract 961207 for the operation of PEPE and PEPE data analysis. The work at Los Alamos National Laboratory (LANL) was supported by NASA Contracts WO-9066, WO-9165, and WO-9138 in the building of PEPE as well as support for data validation, display, distribution, and analysis. We acknowledge the contributions from the entire PEPE team and ion propulsion diagnostic subsystem team as well as technical support provided by the DS1 mission and the NSTAR project. We acknowledge many helpful discussions with P. C. Liewer (JPL), B. Goldstein (JPL), S. P. Gary (LANL), and I. Katz (Maxwell Laboratories).

References

[1]Carruth, M. (ed.), "Experimental and Analytical Evaluation of Ion Thruster/Spacecraft Interactions," Jet Propulsion Lab., Publication 80-92, California Inst. of Technology, Pasadena, CA, 1981.

[2]Samanta Roy, R. I., Hastings, D. E., and Gatsonis, N. A., "Ion-Thruster Plume Modeling for Backflow Contamination," *Journal of Spacecraft and Rockets*, Vol. 33, No. 4, 1996, pp. 525–534.

[3]Samanta Roy, R. I., Hastings, D. E., and Gatsonis, N. A., "Numerical Study of Spacecraft Contamination and Interactions by Ion-Thruster Effluents," *Journal of Spacecraft and Rockets*, Vol. 33, No. 4, 1996, pp. 535–542.

[4]Wang, J., Brophy, J., and Brinza, D., "Three-Dimensional Simulations of NSTAR Ion Thruster Plasma Environment," AIAA Paper 96-3202, July 1996.

[5]Kerslake, W., Goldman, R., and Nieberding, W., "SERT II: Mission, Thruster Performance, and In-Flight Thrust Measurements, *Journal of Spacecraft and Rockets*, Vol. 8, No. 3, 1971, pp. 213–224.

[6]Jones, S., Staskus, J., and Byers, D., "Preliminary Results of SERT II Spacecraft Potential Measurements," NASA TM X-2083, 1970.

[7]Worlock, R., James, E., Hunter, R., and Bartlett, R., "ATS-6 Cesium Bombardment Engine North–South Stationkeeping Experiment," *IEEE Transactions on Aerospace and Electronic Systems*, Vol. 11, No. 6, 1975, pp. 1176–1183.

[8]Wang, J., and Brophy, J., "Three-Dimensional Monte Carlo Particle-in-Cell Simulations of Ion Thruster Plumes," AIAA Paper 95-2826, July 1995.

[9]Brinza, D., Wang, J., Polk, J., and Henry, M., "Deep Space One Investigations of Ion Propulsion Contamination: Overview and Initial Results," AIAA Paper 2000-0465, Jan. 2000.

[10]Rayman, M., and Lehman, D., "Deep Space One: NASA's First Deep-Space Technology Validation Mission," *Acta Astronautica*, Vol. 41, No. 4, 1997, pp. 289–299.

[11]Polk, J., Kakuda, R., Anderson, J., Brophy, J., Rawlin, V., Patterson, M., Sovey, J., and Hamley, J., "Validation of the NSTAR Ion Propulsion System on the Deep Space One Mission: Overview and Initial Results," AIAA Paper 99-2274, June 1999.

[12]Rapp, D., and Francis, W., "Charge-Exchange Between Gaseous Ions and Atoms," *Journal of Chemical Physics*, Vol. 37, No. 11, 1962, pp. 2631–2645.

[13]Katz, I., Davis, V., Wang, J., and Brinza, D., "Electrical Potentials in the NSTAR Charge-Exchange Plume," International Electric Propulsion Conf., IEPC Paper 97-042, Cleveland, OH, Aug. 1997.

[14]Gardner, B., Katz, I., and Davis, V., "Predictions of NSTAR Charge-Exchange Ions and Contamination Backflow," International Electric Propulsion Conf., IEPC Paper 97-043, Cleveland, OH, Aug. 1997.

[15]VanGilder, D., Font, G., and Boyd, I., "Hybrid Monte Carlo Particle-in-Cell Simulation of an Ion Thruster Plume," International Electric Propulsion Conf., IEPC Paper 97-182, Cleveland, OH, Aug. 1997.

[16]Chung, P., Talbot, L., and Touryan, K., *Electric Probes in Stationary and Flowing Plasmas*, Springer-Verlag, Berlin, 1979.

A. C. Tribble
Associate Editor

Color reproductions courtesy of the Jet Propulsion Laboratory.